Proceedings of the 21st ICSMGE, Vienna, Austria, 14 – 19 June 2026. Pistrol, Adam & Schweiger (eds.)
Published by: ÖGG, Austrian Society for Geomechanics, Salzburg, Austria, ISBN 978-3-9503898-4-5
https://doi.org/10.53243/ICSMGE2026-868

Numerical analysis on CPT and pile installation in spatially variable clays

Shujin Zhou, Wangcheng Zhang, Martí Lloret-Cabot, Ashraf S. Osman
Department of Engineering, Durham University, United Kingdom, shujin.zhou@durham.ac.uk

Jonathan Nuttall
Deltares, Delft, the Netherlands.

ABSTRACT: Accurately predicting the installation resistance of piles is important for their design and application. The cone penetration test (CPT) is the most widely used in situ sounding tests for pile drivability analysis and capacity prediction. While there are established empirical correlation methods to connect CPT data with pile installation resistance, the underlying mechanisms behind these correlations have yet to be fully understood. This study performs a numerical analysis to investigate the uncertainty of using the soil properties at the pile centre for a large-diameter pile installation prediction. The pile installation and cone penetration processes are modelled using a large-deformation finite-element method considering soil spatial variability. The mechanisms of these two penetration processes are visualised and compared through numerical modelling, and the penetration resistances are compared with existing design methods, including the mechanism-based method and the CPT-based method.

KEYWORDS: Cone penetration test, pile installation, soil spatial variability, large deformation finite element analysis.

1 INTRODUCTION

Pile foundation is one of the most commonly used foundation types in the offshore wind industry (Negro et al., 2017). Large-diameter piles, such as bucket foundations, with an aspect ratio between 0.5 and 10, are popularly employed in offshore practice as an intermediate offshore foundation, offering an alternative to deep piled foundation (Kay et al., 2021).

Pile drivability assessment is vital for offshore wind due to the high pile installation cost (Guo et al., 2022). Reliable prediction of installation resistance is also essential for the effective design and performance of pile foundations. Existing approaches to determine the pile penetration resistance in soils mainly include the mechanism-based method (Houlsby and Byrne, 2005a; Houlsby and Byrne, 2005b) and the cone penetration test (CPT)-based method (Jardine et al., 2005; DNV, 2017).

Site-specific pile design typically relies on information from geotechnical site investigation data. Design values are generally derived under the assumption that the soil at the pile location is spatially uniform (Cai et al., 2021). In reality, however, soil properties (e.g., undrained shear strength, friction angle, relative density, water content) spatially vary in both vertical and horizontal directions due to a combination of geologic, environmental, and physical-chemical factors (Griffiths et al., 2002). A limitation of assuming a uniform soil in design is that it overlooks the inherent spatial variability of soil within the zone influenced by the foundation. This can be particularly critical for large-diameter piles, where the soil characteristics measured at selected locations, e.g. the pile centre from a CPT, may differ considerably from those along the shaft.

This paper investigates the effectiveness of using the soil properties at the pile centre to predict the penetration resistance for a large-diameter pile. The analysis combines 3D large-deformation finite-element (LDFE) modelling with random field theory, applied to both CPT and pile installation simulations. Due to the high computation cost of the numerical modelling, only one single realisation is performed for each scenario.

2 NUMERICAL MODELLING

2.1 *LDFE analysis*

Numerical simulation of cone or pile installation process is a challenge due to the large deformation involved within displaced soils. In this study, the RITSS method (Remeshing and interpolation technique with small strain (Hu and Randolph, 1998)) that falls in the category of Arbitrary Lagrangian Eulerian (ALE) method, is employed and integrated into the commercial software ABAQUS. The installation process is divided into a series of incremental updated Lagrangian (UL) analyses combined with frequent remeshing of the entire domain and remapping field variables. Numerical modelling of large deformation problems in spatially variable soils is computationally challenging precisely because of the coupling of large deformations and soil variability. Recent studies (Zhang et al., 2022; Zhou et al., 2026) showed that frequent remeshing and interpolation introduce errors and modify the original random field, and they used a set of dummy material points to store the random field to mitigate error accumulation. The same strategy is used here for 3D simulation, but the positions of material points are not updated (i.e., the random field is fixed) to reduce computation time. The effect of material redistribution is expected to be minimal for cone tip resistance and the penetration behaviour of a large-diameter unplugged pile.

2.2 *Random field model*

The inherent soil variability can be described with random field theory, with the mean (μ), coefficient of variation (COV), and correlation length or scale of fluctuation (θ). In this study, only the undrained shear strength s_u is treated as a random variable and, to prevent negative values, is characterised by a lognormal distribution. A standard normally distributed random field $G(x)$ is first obtained using the Local Average Subdivision (LAS) method (Fenton and Vanmarcke, 1990), and then converted into a lognormal field following Griffiths and Fenton (2001):

$$s_{ui} = \exp\left(\mu_{\ln(s_u)} + \sigma_{\ln(s_u)} \cdot G(x_i)\right) \quad (1)$$

where s_{ui} is the undrained shear strength assigned to the ith cell; x_i is a vector containing the coordinates of the centre of ith cell; $\mu_{\ln(s_u)}$ and $\sigma_{\ln(s_u)}$ are the mean and standard deviation of the logarithm of undrained shear strength, which can be obtained through Equation (2) and Equation (3), respectively.

$$\sigma_{\ln(s_u)} = \sqrt{\ln\left(1 + \mathrm{COV}_{s_u}{}^2\right)} \quad (2)$$

$$\mu_{\ln(s_u)} = \ln\left(\mu_{s_u}\right) - \frac{1}{2}\sigma_{\ln(s_u)}{}^2 \quad (3)$$

The scale of fluctuation θ is a fundamental parameter in the correlation model that characterises the spatial variability within a random field (e.g., Lloret-Cabot et al., 2014). The

Markov correlation function is used to generate the random field, and is expressed by:

$$\rho(\tau) = \exp\left(\frac{-2|\tau|}{\theta}\right) \quad (4)$$

where $\rho(\tau)$ is the correlation function, and τ is the distance between two points.

2.3 *Geometry and parameters*

In this study, a CPT is conducted at the centre of a large-diameter pile, as shown in Figure 1. The CPT data are used to estimate the pile's penetration resistance. However, due to soil spatial variability, the CPT profile at the pile centre may differ from those along the shaft, leading to potential discrepancies between the resistance predicted from the centre CPT and the actual resistance. Both the CPT and the pile installation are simulated using numerical modelling.

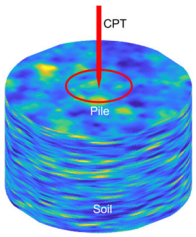

Figure 1. Schematic diagram of CPT and pile penetration.

The piezocone model has a cone area of 1500 mm^2 (diameter D_c = 43.7 mm) and a tip–apex angle of 60°. Both cone tip resistance, q_c, and sleeve friction, f_s, can be obtained from the numerical modelling, but only cone tip resistance is used in this study. The pipe pile of a diameter D_p = 8.0 m, a length L = 8 m (i.e., L/D_p = 1.0), a wall thickness t = 0.1 m (i.e., D_p/t = 80) is considered in the numerical modelling. These dimensions are typical for offshore large-diameter pile foundations (Stapelfeldt et al., 2018). The pile and the cone are simplified as rigid bodies since their stiffness greatly exceeds that of the soil.

As shown in Figure 2, a cylindrical soil domain with a radius of 2.5 m and a depth of 11 m is modelled for CPT simulation; while for pile installation, a domain of 25 m in radius and 25 m in depth is used to ensure that the domain boundaries are well outside the soil plastic zone. Hinge and roller supports are assumed along the base and radial sides of the soil domain, respectively. Eight-node linear brick elements (C3D8) are used in the FE analysis.

The soil is modelled as a linear elastic-perfectly plastic material obeying a Tresca yield criterion. The mean undrained soil strength is taken as μ_{s_u} = 10 kPa with a Poisson's ratio of ν = 0.495 and the Young's modulus $E = 300s_u$. The effects of soil stiffness on the tip resistance have been studied by Zhou et al. (2024), and a representative value is adopted here based on McCarron (2024).

The pile-soil contact plays an important role in bearing capacity and penetration resistance estimation. In this study, the α method is used whereby the pile-soil shear stress governed by Coulomb's friction law is capped by the maximum value $\tau_{max} = \alpha s_u$, where α is the adhesion factor, typically ranging from 0.1 to 1 (Karlsrud, 2014), and taken as 0.5 in this study.

A larger square prism random field domain of a width of 50 m and a depth of 30 m is generated using LAS (Hicks et al., 2014), while only part of the random field is used in the FE model. The random field domain should be larger than the FE model to maintain the accuracy after interpolation (Zhang et al., 2022; Zhou et al., 2025). The input random field statistics for the undrained shear strength, COV = 0.3 and θ_v = 1 m, are used. Three horizontal correlation lengths, θ_h = 1 m, 8 m, and 80 m, are considered to investigate the effect of spatial variability of s_u within the zone influenced by the foundation, as illustrated in Figure 3. These parameter values are within the typical range observed in natural soils (Phoon and Kulhawy, 1999).

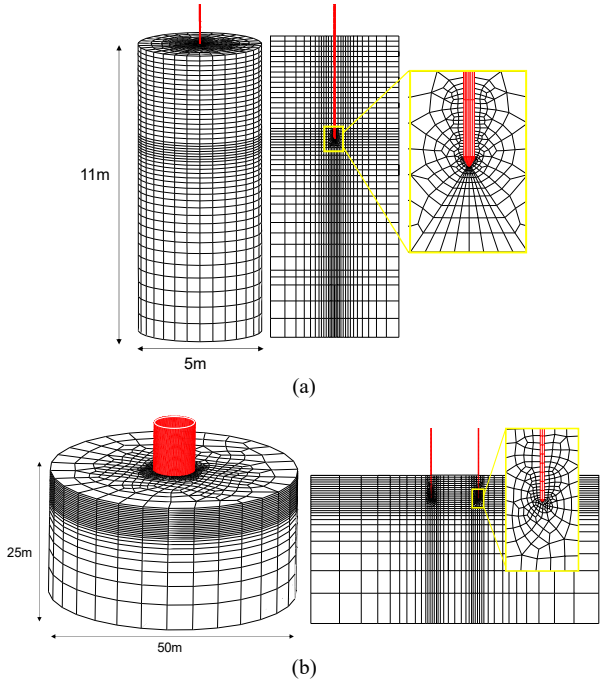

Figure 2. Numerical model: (a) CPT; (b) pile.

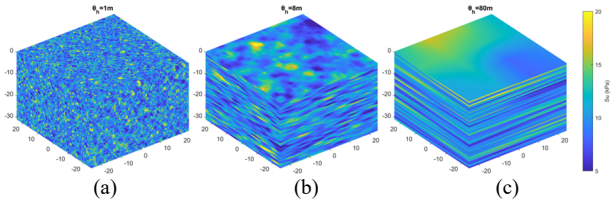

Figure 3. Generated 3D random fields (50 m × 50 m × 30 m) according to different horizontal correlation lengths (COV = 0.3, θ_v = 1 m): (a) θ_h = 1 m; (b) θ_h = 8 m; (c) θ_h = 80 m.

3 RESULTS AND DISCUSSION

3.1 *Failure mechanism in spatially variable soils*

The spatial variability of soil properties has a significant influence on the penetration behaviour of both CPT and piles. To demonstrate this, Figure 4 and Figure 5 present an example case with a horizontal correlation length (θ_h) of 8 m, illustrating the failure mechanisms during cone and pile penetration, respectively.

Figure 4 shows the soil flow mechanism for CPT penetration, with Figure 4a for the contours of soil strength and regions of plastic yielding (in grey colour), and Figure 4b showing the distribution of maximum shear stress ($(\sigma_1 - \sigma_3)/2$, where σ_1 and σ_3 are the maximum and minimum principal stresses, respectively). Similarly, the random field of s_u and maximum shear stress distribution for pile installation are shown in Figure 5a and 5b, respectively. The results indicate that in spatially heterogeneous ground, the mobilised soil regions for pile become asymmetric due to the tendency of the failure mechanism to follow the weakest path (see also Griffiths et al., 2002; Zhang et al., 2022). Nonetheless, the shear band formed during cone penetration appears more symmetric. This is because the locally mobilised zone by a relatively small size of cone to the pile exhibits relatively uniform spatial variability. For example, in homogeneous clay

with $E/s_u = 300$, cone penetration causes plastic deformation in a zone of soil extending approximately 5 to 8 cone radii (i.e., 0.11 ~ 0.17 m) (Lu et al., 2004). When the soil has a vertical correlation length θ_v= 1 m and horizontal correlation length θ_h= 8 m, the variability within this localised zone remains relatively consistent.

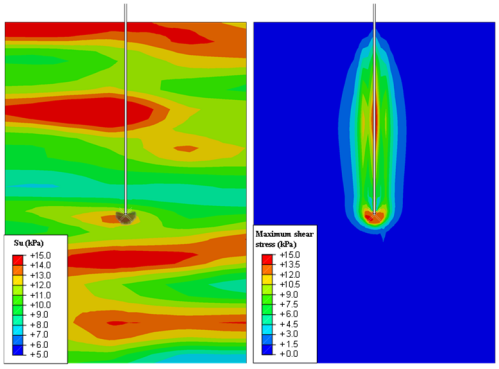

(a) (b)

Figure 4. Failure mechanism for cone penetration (d = 4 m): (a) s_u distribution; (b) maximum shear stress.

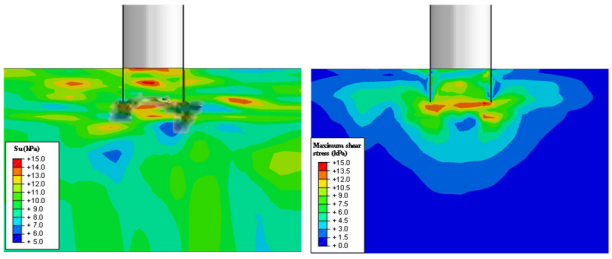

(a) (b)

Figure 5. Failure mechanism for pile penetration (d = 4 m): (a) s_u distribution; (b) maximum shear stress.

3.2 *Penetration resistances*

3.2.1 *Mechanism-based method*

For clay deposits, the cone factor N_{kt} is used to correlate the net cone tip resistance q_{net} to the undrained shear strength s_u as

$$N_{kt} = \frac{q_{net}}{s_u} = \frac{q_c - \sigma_{v0}}{s_u} \quad (5)$$

where q_c is the cone tip resistance; σ_{v0} is the overburden stress at the cone tip level. Typical ranges of cone factor, N_{kt}, may be found in the literature (Lunne et al., 2002), and vary from as low as 6 to above 20. To determine a proper cone factor to interpret the cone resistance, a deterministic numerical analysis with s_u = 10 kPa is conducted. Figure 6a presents the net cone tip resistance (q_{net}) profile from the uniform case. Based on Equation (5), the corresponding cone factor N_{kt} = 11.4 is derived. The undrained shear strength estimated from the simulated CPT can then be calculated and is illustrated in Figure 6b.

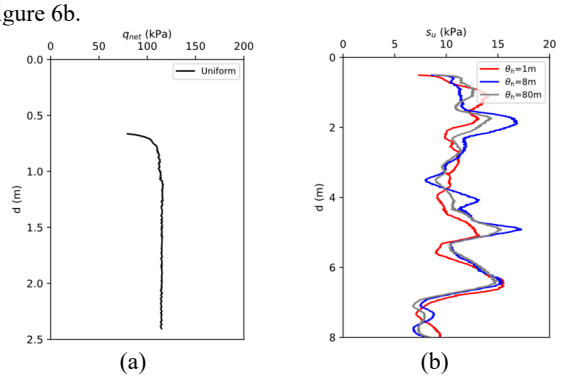

(a) (b)

Figure 6. CPT interpretation: (a) cone tip resistance from uniform soil; (b) CPT-measured s_u.

Mechanism-based prediction method of pile penetration resistance in clay using the bearing capacity theory has been proposed by Houlsby and Byrne (2005a):

$$F = \alpha s_{u,av} A_s + \left(N_c s_{u,t} + \gamma' d\right) A_t \quad (6)$$

where F is the total resistance; α is the adhesion factor; $s_{u,av}$ is the average shear strength of soil over the penetration depth, d; $s_{u,t}$ is the shear strength of soil at the pile tip level; N_c is the bearing capacity factor; γ' is the effective unit weight; A_s and A_t are the pile wall area and tip area, respectively.

The penetration resistances based on the CPT-measured s_u at the pile centre are calculated using Equation (6) with N_c = 11.4 and α = 0.5, and are referred to as F_{design}. These values are compared to the total resistances obtained from numerical modelling (F_{actual}), as shown in Figure 7a. To highlight the relative difference between the design approach and the actual resistance, the ratios F_{design}/F_{actual} are presented in Figure 7b. The results indicate that the design method tends to overestimate penetration resistance in these three cases, particularly at shallow depths. The difference between shallow and deep depths arises because tip resistance, which dominates in shallow layers, is highly influenced by local spatial variability. As the pile penetrates deeper, shaft resistance becomes more significant. Since shaft resistance reflects the average spatial variability, it exhibits less fluctuation with depth. It should be noted that in the numerical simulation, zero or smaller than αs_u interface strength may develop at shallow depths due to the formation of a tension or a gap zone, especially in the external shaft, which increases the ratio of F_{design}/F_{actual}. Also, N_c used in the pile tip resistance prediction is not conservative (valued at 11.4 based on CPT), whereas in design practice N_c = 9 is commonly used. The prediction also depends on the pattern of spatial variation.

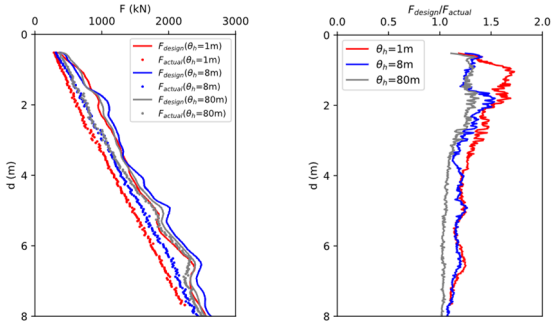

(a) (b)

Figure 7. Resistance prediction using mechanism-based method: (a) penetration resistance F_{design} and F_{actual}; (b) the ratios F_{design}/F_{actual}.

3.2.2 *CPT-based method*

A direct CPT-based design method was proposed by Det Norske Veritas (DNV, 2017), where both the tip resistance and wall friction are related to the CPT tip resistance, i.e.

$$F = k_p(d) A_t q_c + A_s' \int_0^d k_f(z) q_c(z)\, dz \quad (7)$$

where $k_p(d)$ = empirical coefficient relating q_c to pile end resistance during installation, ranging from 0.4 to 0.6 for clay; $k_f(z)$ = empirical coefficient relating q_c to pile skin friction, ranging from 0.03 to 0.05 for clay; A_s' is the side area of penetrating member, per unit penetration depth.

Based on the guidance provided by Det Norske Veritas (DNV, 2017), a most probable (where lower limits of coefficients are used, i.e. k_p = 0.4, k_f = 0.03) and a highest

expected (k_p = 0.6, k_f = 0.05) penetration resistance, F_{prob} and F_{max}, respectively, can be calculated and shown in Figure 8. It can be seen that the actual resistance from numerical modelling is close to F_{max} at shallow depths, and gradually falls within the range between F_{prob} and F_{max} as depth increases. In addition to the significant uncertainty at shallow depths, the actual value of k_f also varies with adhesion factor and depth as:

$$k_f = \frac{\alpha s_u}{N_{kt} s_u + \gamma' d} \quad (8)$$

which gives k_f = 0.044 at d = 0 m and k_f = 0.031 at d = 8 m using deterministic values of α = 0.5, s_u = 10 kPa, N_{kt} = 11.4, and γ' = 5.88 kN/m^3.

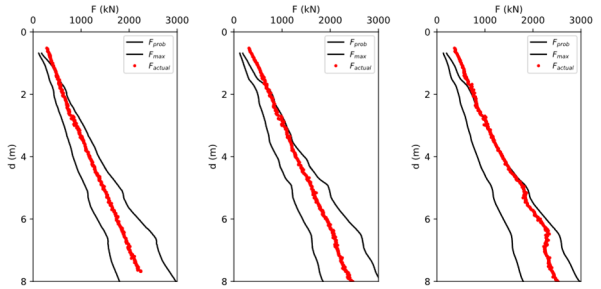

(a) (b) (c)

Figure 8. Resistance prediction using CPT-based method: (a) θ_h = 1 m; (b) θ_h = 8 m; (c) θ_h = 80 m.

4 CONCLUSIONS

Existing design approach for large-diameter pile installation prediction overlooks the inherent spatial variability of soil within the zone influenced by the foundation. To assess its accuracy, a 3D large deformation numerical analysis is carried out to evaluate both the mechanism-based and CPT-based methods, using the soil profile at the pile centre to estimate installation resistance. These predictions are then compared with the numerical simulation results. It is found that the predicted resistance is less reliable in shallow depth than in deep depth using the mechanism-based method. Using the CPT-based method, the actual resistance lies close to the maximum resistance at shallow depths and gradually falls within the suggested range from the most probable resistance to the maximum resistance as depth increases.

Note that the above discussions are based on the results from one realisation for each case; further studies with Monte Carlo analysis are required to validate more fully the reliability of these design methods.

5 ACKNOWLEDGEMENTS

The first author would like to acknowledge the supports of Research Training Support Grant from Department of Engineering, Durham University.

6 REFERENCES

Cai, Y., Bransby, F., Gaudin, C. & Uzielli, M. 2021. A framework for the design of vertically loaded piles in spatially variable soil. *Computers and Geotechnics* 134:104140.

Dnv, G. 2017. Offshore soil mechanics and geotechnical engineering. *Offshore Standard DNVGL-RP-C212, Edition August*.

Fenton, G. A. & Vanmarcke, E. H. 1990. Simulation of random fields via local average subdivision. *Journal of Engineering Mechanics* 116(8):1733-1749.

Griffiths, D. & Fenton, G. A. 2001. Bearing capacity of spatially random soil: the undrained clay Prandtl problem revisited. *Geotechnique* 51(4):351-359.

Griffiths, D., Fenton, G. A. & Manoharan, N. 2002. Bearing capacity of rough rigid strip footing on cohesive soil: Probabilistic study. *Journal of Geotechnical and Geoenvironmental Engineering* 128(9):743-755.

Guo, Y., Wang, H. & Lian, J. 2022. Review of integrated installation technologies for offshore wind turbines: Current progress and future development trends. *Energy Conversion and Management* 255:115319.

Hicks, M. A., Nuttall, J. D. & Chen, J. 2014. Influence of heterogeneity on 3D slope reliability and failure consequence. *Computers and Geotechnics* 61:198-208.

Houlsby, G. T. & Byrne, B. W. 2005a. Design procedures for installation of suction caissons in clay and other materials. *Proceedings of the Institution of Civil Engineers-Geotechnical Engineering* 158(2):75-82.

Houlsby, G. T. & Byrne, B. W. 2005b. Design procedures for installation of suction caissons in sand. *Proceedings of the Institution of Civil Engineers-Geotechnical Engineering* 158(3):135-144.

Hu, Y. & Randolph, M. 1998. A practical numerical approach for large deformation problems in soil. *International Journal for Numerical and Analytical Methods in Geomechanics* 22(5):327-350.

Jardine, R., Chow, F., Overy, R. & Standing, J. 2005. *ICP design methods for driven piles in sands and clays.* Thomas Telford London.

Karlsrud, K. 2014. Ultimate shaft friction and load-displacement response of axially loaded piles in clay based on instrumented pile tests. *Journal of Geotechnical and Geoenvironmental Engineering* 140(12):04014074.

Kay, S., Gourvenec, S., Palix, E. & Alderlieste, E. 2021. *Intermediate offshore foundations.* CRC press.

Lloret-Cabot, M., Fenton, G. A. & Hicks, M. A. 2014. On the estimation of scale of fluctuation in geostatistics. *Georisk: Assessment and management of risk for engineered systems and geohazards* 8(2):129-140.

Lu, Q., Randolph, M., Hu, Y. & Bugarski, I. 2004. A numerical study of cone penetration in clay. *Geotechnique* 54(4):257-267.

Lunne, T., Powell, J. J. & Robertson, P. K. 2002. *Cone penetration testing in geotechnical practice.* CRC press.

McCarron, W. 2024. Modelling pile foundations under biaxial loading with a plasticity-based p–y methodology. *Canadian Geotechnical Journal* 62:1-13.

Negro, V., López-Gutiérrez, J.-S., Esteban, M. D., Alberdi, P., Imaz, M. & Serraclara, J.-M. 2017. Monopiles in offshore wind: Preliminary estimate of main dimensions. *Ocean Engineering* 133:253-261.

Phoon, K.-K. & Kulhawy, F. H. 1999. Characterization of geotechnical variability. *Canadian Geotechnical Journal* 36(4):612-624.

Stapelfeldt, M., Bienen, B. & Grabe, J. 2018. Centrifuge tests investigating the effect of suction caisson installation in dense sand on the state of the soil plug. In *Physical Modelling in Geotechnics, Volume 1.*) CRC Press, pp. 669-674.

Zhang, W., Pan, Y. & Bransby, F. 2022. Scale effects during cone penetration in spatially variable clays. *Geotechnique* 72(1):78-90.

Zhou, S., Zhang, W., Lloret-Cabot, M. & Osman, A. S. 2026. An interpolation and remesh based large deformation finite element method considering soil spatial variability. *Computers and Geotechnics* 190:107732.

Zhou, S., Zhang, W. & Osman, A. S. 2024. Effect of soil stiffness on end bearing resistance of foundations in clay from large deformation numerical modelling. *Computers and Geotechnics* 173:106515.